

Anomalous resistivity and superconductivity in the two-band Hubbard model with one narrow band (Review)

Cite as: *Low Temp. Phys.* **37**, 69 (2011); <https://doi.org/10.1063/1.3552118>
 Published Online: 10 February 2011

M. Yu. Kagan, and V. V. Valkov



View Online



Export Citation

ARTICLES YOU MAY BE INTERESTED IN

[Strongly Correlated Materials: Insights From Dynamical Mean-Field Theory](#)
Physics Today **57**, 53 (2004); <https://doi.org/10.1063/1.1712502>



MONTANA INSTRUMENTS

QUANTUM COMPUTING SPINTRONICS : MOKE DIAMOND NV CENTERS

CLICK HERE
CRYOGENIC
 APPLICATION
 NOTES

montanainstruments.com/Applications/Application-Notes/

COLD SCIENCE MADE SIMPLE

Anomalous resistivity and superconductivity in the two-band Hubbard model with one narrow band (Review)

M. Yu. Kagan

P. L. Kapitza Institute for Physical Problems of the Russian Academy of Sciences, 2 Kosygin St., Moscow 119334, Russia

V. V. Valkov

Kirensky Institute of Physics, Siberian Branch of the Russian Academy of Sciences, Akademgorodok, Krasnoyarsk 660036, Russia

(Submitted September 7, 2010)

Fiz. Nizk. Temp. **37**, 84–99 (January 2011)

We search for marginal Fermi-liquid behavior in the two-band Hubbard model with one narrow band. We consider the limit of low electron densities in the bands and strong intraband and interband Hubbard interactions. We analyze the influence of electron-polaron effects and other mechanisms for mass-enhancement (related to the momentum dependence of the self-energies) on the effective mass and scattering times of light and heavy components in the clean case (electron-electron scattering and no impurities). We find a tendency towards phase separation (towards negative partial compressibility of heavy particles) in the 3D case with a large mismatch between the densities of heavy and light bands in the strong coupling limit. We also find that for low temperatures and equal densities, the resistivity in a homogeneous state $R(T) \propto T^2$ behaves as a Fermi-liquid in both 3D and 2D. For temperatures greater than the effective bandwidth for heavy electrons $T > W_h^*$, the coherence of the heavy component breaks down completely. The heavy particles move diffusively in the surrounding light particles. At the same time, light particles scatter on heavy particles as if on immobile (static) impurities. Under these conditions, the heavy component is marginal, while the light component is not. The resistivity approaches saturation for $T > W_h^*$ in the 3D case. In 2D the resistivity has a maximum and a localization tail owing to weak-localization corrections of the Altshuler-Aronov type. This behavior of resistivity in 3D could be relevant for some uranium-based heavy-fermion compounds such as UNi_2Al_3 and in 2D, for some other mixed-valence compounds, possibly including layered magnetites. We also consider briefly the superconductive (SC) instability in this model. The leading instability tends to p -wave pairing and is governed by an enhanced Kohn–Luttinger mechanism for SC at low electron densities. The critical temperature corresponds to the pairing of heavy electrons via polarization of the light electrons in 2D. © 2011 American Institute of Physics. [doi:10.1063/1.3552118]

Dedicated to the memory of Prof. David Shoenberg

I. INTRODUCTION

The physics of uranium-based heavy-fermion compounds and the origin of a heavy mass $m_h^* \sim 200m_e$ in them may be very different (see¹) from the physics of cerium-based heavy-fermions, where the Kondo-effect is dominant.^{2,3} The essential point is that uranium-based heavy fermions are usually in the mixed valence limit⁴ with strong hybridization between heavy and light components. On the level of two-particle hybridization, the interband Hubbard interaction leads to an additional enhancement of the heavy electrons' mass owing to the electron-polaron effect (EPE). Physically EPE is connected with a nonadiabatic part of the many-body wave function describing a heavy electron and a cloud of virtual electron-hole pairs of light electrons. These pairs are mixed with the wave function of the heavy electrons but do not follow it when a heavy electron tunnels from one elementary cell to a neighboring one. In the unitary limit of the strong Hubbard interaction between heavy and light electrons¹ the effective heavy mass could reach m_h^*/m_l

$\sim (m_h/m_l)^2$. If we start with a ratio $m_h/m_l \sim 10$ of the bare masses of heavy and light electrons, on the level of local-density approximation (LDA), for example, we could finish with an effective value $m_h^* \sim 100m_l$, which is typical for uranium based heavy-fermion compounds.

This kind of effect could also be described in terms of strong one-particle hybridization between heavy and light bands.¹

A natural question arises: is the two-band Hubbard model with one narrow band just a simple toy-model for observing non-Fermi-liquid behavior and, in particular, the well known marginal Fermi-liquid behavior?⁵ Recall that in the theory of marginal Fermi-liquids (MFL) the quasiparticles are strongly damped ($\text{Im } \epsilon \sim \text{Re } \epsilon \sim T$). Strong damping $\gamma \propto T$ of the quasiparticles (instead of a standard damping for Landau Fermi-liquid picture $\gamma \propto T^2/\epsilon_F$) could explain⁵ a number of observations in HTSC compounds, including a linear resistivity $R(T) \propto T$ for $T > T_c$ at optimal doping con-

centrations. The MFL picture was also proposed to describe the properties of UPt₃ doped with Pd, including its specific heat.⁶

Here we evaluate the damping and transport times for heavy and light electrons. We verify these times and find that at low temperatures $T < W_h^*$, the effective bandwidth for heavy electrons and equal densities of heavy and light bands in a homogeneous state, we have the standard behavior of a Landau Fermi-liquid with resistivity $R(T) \propto T^2$ for the case of electron-electron scattering in both 3D and 2D. For higher temperatures $T > W_h^*$ ($W_h^* \sim 50$ K for $m_h^* \sim 200m_e$) the heavy band is totally destroyed and the heavy particles move diffusively in the surrounding of light particles while the light particles scatter on the heavy ones as if on immobile (static) impurities. For these temperatures the heavy component is marginal, while the light component is not. We try to make a light component marginal by considering weak localization corrections of Altshuler-Aronov type⁷ for the scattering time of light electrons. We do not get marginal behavior of light component, but we get some very interesting anomalous resistivity characteristics, especially in the 2D case, where for $T \sim W_h^*$ the resistivity has a maximum and a localization tail at higher temperatures.⁸ In 3D the resistivity approaches saturation as $T > W_h^*$. Resistivity characteristics of this sort could possibly describe some 3D uranium-based heavy-fermion compounds such as UNi₂Al₃ and some other mixed-valence systems. In 2D the resistivity behavior may have some relation to layered manganites where we deal with two degenerate (e_g) conducting orbitals (bands) of d -electrons of Mn. However, for manganites an alternative explanation is possible:⁹ the resistivity is governed by electron tunneling from one metallic FM polaron to a neighboring one via an insulating AFM or PM barrier in a nanoscale phase separation regime for the electronic subsystem. It will be interesting to compare these two mechanisms for resistivity in layered manganites more accurately.

We also consider mechanisms of heavy-mass enhancement other than EPE and find a very pronounced effect in 3D connected with the momentum dependence of the self-energy of heavy electrons owing to the "heavy-light" interaction. In a strong coupling limit this effect could provide even larger ratios of m_h^*/m_h than EPE. It leads to a negative compressibility for the heavy particles and thus reveals a tendency towards phase-separation or at least charge redistribution between the bands with a large density mismatch $n_h \gg n_l$, in qualitative agreement with the results of Ref. 10.

In the final section of this paper we study the leading SC instability which develops in the 2D two-band model. The leading instability at low density is triplet p -wave pairing. This describes the pairing of heavy electrons via polarization of light electrons^{11,12} in the framework of an enhanced Kohn-Luttinger¹³ mechanism for SC and provides rather realistic critical temperatures in the 2D or layered case, especially when the geometrically separated bands belonging to neighboring layers.

II. THE TWO-BAND HUBBARD MODEL WITH ONE NARROW BAND

The Hamiltonian for the two-band Hubbard model is

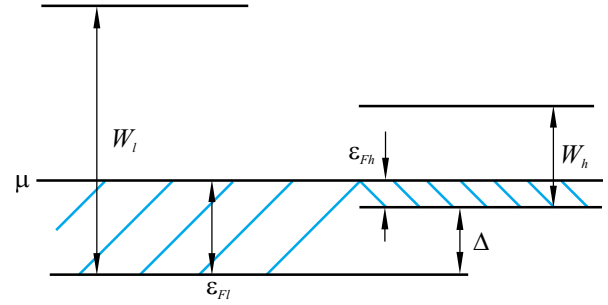


FIG. 1. The band structure in the two-band model with one narrow band. W_h and W_l are the bandwidths of heavy and light electrons, ε_{Fh} and ε_{Fl} are the Fermi energies, Δ is the energy difference between the bottoms of the heavy and light bands, and μ is chemical potential.

$$\hat{H}' = -t_h \sum_{\langle ij \rangle \sigma} a_{i\sigma}^+ a_{j\sigma} - t_l \sum_{\langle ij \rangle \sigma} b_{i\sigma}^+ b_{j\sigma} + \Delta \sum_{i\sigma} n_{i\sigma}^\sigma - \mu \sum_{i\sigma} (n_{i\sigma}^L + n_{i\sigma}^h) + U_{hh} \sum_i n_{ih}^\uparrow n_{ih}^\downarrow + U_{ll} \sum_i n_{il}^\uparrow n_{il}^\downarrow + \frac{U_{hl}}{2} \sum_i n_{ih} n_{il}, \quad (1)$$

where U_{hh} and U_{ll} are intraband Hubbard interactions for heavy and light electrons respectively, U_{hl} is the interband Hubbard interaction between heavy and light electrons, t_h and t_l are the transfer integrals for heavy and light electrons, $n_{ih}^\sigma = a_{i\sigma}^+ a_{i\sigma}$ and $n_{il}^\sigma = b_{i\sigma}^+ b_{i\sigma}$ are the densities of heavy and light electrons on site i with spin-projection σ , μ is the chemical potential, and Δ is the difference between the bottoms of the bands. Taking the Fourier transform, we get

$$\hat{H}' = \sum_{p\sigma} \varepsilon_h(p) a_{p\sigma}^+ a_{p\sigma} + \sum_{p\sigma} \varepsilon_l(p) b_{p\sigma}^+ b_{p\sigma} + U_{hh} \sum_{pp'q} a_{p\uparrow}^+ a_{p'\downarrow}^+ a_{p-q\downarrow} a_{p'+q\uparrow} + U_{ll} \sum_{pp'q} b_{p\uparrow}^+ b_{p'\downarrow}^+ b_{p-q\downarrow} b_{p'+q\uparrow} + \frac{U_{hl}}{2} \sum_{pp'q} a_{p\sigma}^+ (b_{p'\sigma'}^+ b_{p-q\sigma'}) a_{p'+q\sigma}, \quad (2)$$

where

$$\varepsilon_h(p) = -2t_h \sum_{a=1}^D \cos(p_a d) - \varepsilon_0 - \mu, \\ \varepsilon_l(p) = -2t_l \sum_{a=1}^D \cos(p_a d) - \mu$$

are the quasiparticle energies for heavy and light bands in D -dimensions for the hypercubic lattice (see Fig. 1), and $p_a = \{p_x, p_y, \dots\}$ are Cartesian projections of the momentum. For low densities of heavy and light components such that $n_{\text{tot}} d^D = (n_h + n_l) d^D \ll 1$, the quasiparticle spectra are

$$\varepsilon_h(p) = -\frac{W_h}{2} + t_h(p^2 d^2) - \varepsilon_0 - \mu;$$

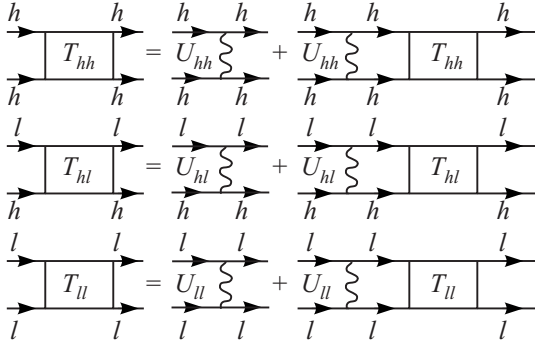


FIG. 2. The T -matrices T_{hh} , T_{ll} , and T_{hl} for the two-band model with heavy (h) and light (l) electrons.

$$\varepsilon_l(p) = -\frac{W_l}{2} + t_l(p^2 d^2) - \mu, \quad (3)$$

where $W_h = 4D_{th}$ and $W_l = 4D_{tl}$ are the bandwidths of heavy and light electrons for a D -dimensional hypercubic lattice, and d is the intersite distance. On introducing the bare masses of the heavy and light components,

$$m_h = \frac{1}{2t_h d^2}; \quad m_l = \frac{1}{2t_l d^2} \quad (4)$$

and the Fermi energies

$$\varepsilon_{Fh} = \frac{p_{Fh}^2}{2m_h} = \frac{W_h}{2} + \mu + \varepsilon_0; \quad \varepsilon_{Fl} = \frac{W_l}{2} + \mu, \quad (5)$$

we get the quasiparticle spectra for $T \rightarrow 0$

$$\varepsilon_h(p) = \frac{p^2}{2m_h} - \varepsilon_{Fh}; \quad \varepsilon_l(p) = \frac{p^2}{2m_l} - \varepsilon_{Fl}. \quad (6)$$

In deriving Eqs. (4)–(6) we implicitly assume that the difference between the bottom of the bands, Δ , in Fig. 1 is not too large, so a parabolic approximation for the spectra of both bands is still valid.

Note that there is no one-particle hybridization in the hamiltonians (1), (2)n but there is a strong two-particle hybridization

$$\frac{U_{hl}}{2} \sum_i n_i^h n_i^l.$$

We assume that $m_h \gg m_l$, so that

$$W_h/W_l = m_l/m_h \ll 1. \quad (7)$$

We also assume that $U_{hh} \sim U_{ll} \sim U_{hl} \gg W_l \gg W_h$, i.e., strong coupling (U_{hl} is large because in reality light particles experience strong scattering on the heavy ones as if on a quiresonance level). Finally we consider the simplest case where the densities of the bands are of the same order: $n_h \sim n_l$ (note that in 3D, $n = pF^3/3\pi^2$, while in 2D $n = pF^2/2\pi$).

III. THE KANAMORI T -MATRIX APPROXIMATION

According to renormalization scheme of Kanamori, for low electron density (practically empty lattice) the strong Hubbard interactions¹⁴ should be replaced by the corresponding vacuum T -matrices (see Fig. 2).

In the 3D case the solution of the corresponding Bethe-Salpeter integral equations in vacuum yields for T -matrices,

$$T_{hh} = \frac{U_{hh} d^3}{1 - U_{hh} d^3 K_{hh}^{\text{vac}}(0,0)} = \frac{U_{hh} d^3}{1 + \frac{U_{hh}}{8\pi t_h}}; \quad (8)$$

$$T_{hl} = \frac{U_{hl} d^3}{1 + \frac{U_{hl}}{8\pi t_{hl}^*}}; \quad T_{ll} = \frac{U_{ll} d^3}{1 + 8\pi t_l},$$

where

$$K_{hh}^{\text{vac}}(0,0) = - \int \frac{d^3 \mathbf{p}}{(2\pi)^3} \frac{m_h}{p^2}$$

is a Cooper loop for heavy particles in vacuum (the product of two vacuum Green functions of heavy particles in a Cooper channel for total frequency and total momentum equal to zero),

$$m_{hl}^* = \frac{1}{2t_{hl}^* d^2} = \frac{m_h m_l}{(m_h + m_l)} \approx m_l$$

for $m_h \gg m_l$ is an effective mass for the T -matrix T_{hl} (for scattering of light electrons on heavy electrons) and accordingly $t_{hl}^* \approx t_l$ is an effective transfer integral; $U d^3$ plays the role of a zeroth order Fourier component in 3D. As a result for $U_{hh} \sim U_{ll} \sim U_{hl} \gg W_l \gg W_h$

$$T_{hh} = 8\pi t_h d^3; \quad T_{hl} \approx T_{ll} \approx 8\pi t_l d^3. \quad (9)$$

The s -wave scattering length for the Hubbard model¹¹ is defined as $a = mT/(4\pi) = T/(8\pi t d^2)$, so that

$$a_{hh} = a_{hl} = a_{ll} = d \quad (10)$$

for strong coupling.

Hence the Galitskii gas parameter $f_0 = 2ap_F/\pi$ ^{15,16} for equal densities of heavy and light bands, $n_l = n_h$, is

$$f_0 = (f_0^l = 2dp_{Fl}/\pi) = (f_0^h = 2dp_{Fh}/\pi) = 2dp_F/\pi. \quad (11)$$

(It is convenient to include the factor $2/\pi$ in the definition of the gas-parameter in 3D.) In the 2D case, for strong Hubbard interactions and low densities, with logarithmic accuracy the vacuum T -matrices for $n_l = n_h$ ^{11,12} are

$$T_{hh} = \frac{U_{hh} d^2}{\left(1 + \frac{U_{hh}}{8\pi t_h} \int_{p_F^2}^{U d^2} \frac{dp^2}{p^2}\right)} = \frac{U_{hh} d^2}{\left(1 + \frac{U_{hh}}{8\pi t_h} \ln \frac{1}{p_F^2 d^2}\right)};$$

$$T_{ll} = \frac{U_{ll} d^2}{\left(1 + \frac{U_{ll}}{8\pi t_l} \ln \frac{1}{p_F^2 d^2}\right)}; \quad T_{hl} \approx \frac{U_{hl} d^2}{\left(1 + \frac{U_{hl}}{8\pi t_l} \ln \frac{1}{p_F^2 d^2}\right)}, \quad (12)$$

where $U d^2$ plays the role of a zeroth order Fourier component of the Hubbard potential in 2D. Thus, for strong coupling the 2D gas parameter of Bloom¹⁷ for equal densities $n_l = n_h$ becomes

$$f_0 = f_{0l} = f_{0h} = \frac{1}{2 \ln(1/p_F d)}. \quad (13)$$

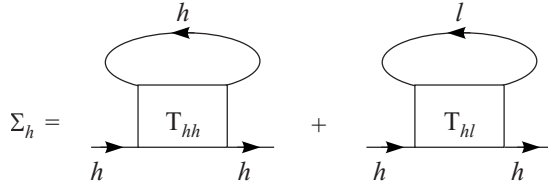


FIG. 3. The T -matrix approximation for the self-energies of a heavy particle. T_{hh} and T_{hl} are the full T -matrices in the material. The diagrams for Σ_l are analogous.

IV. EVALUATING THE SELF-ENERGIES OF HEAVY AND LIGHT BANDS

Let us evaluate the imaginary part of the self-energies $\text{Im } \Sigma$ in a two-band Hubbard model for the clean case (no impurities) and including only electron-electron scattering. It is important for evaluating the scattering times for heavy and light electrons and further calculation of the resistivity $R(T)$.

In the two-band model (see Fig. 3)

$$\Sigma_h = \Sigma_{hh} + \Sigma_{hl} \quad \text{and} \quad \Sigma_l = \Sigma_{ll} + \Sigma_{lh}. \quad (14)$$

The full T -matrices which appear in the diagrams for Σ in Fig. 3 are

$$T_{hh}(\Omega, \mathbf{p}) = \frac{U_{hh}d^3}{1 - U_{hh}d^3 K_{hh}(\Omega, \mathbf{p})}, \quad (15)$$

in the 3D case, where

$$K_{hh}(\Omega, \mathbf{p}) = \int \frac{d^D \mathbf{p}'}{(2\pi)^2} \frac{1 - n_h^F(\varepsilon_{p'+p}) - n_h^F(\varepsilon_{-p'})}{\Omega - \varepsilon_h(p' + p) - \varepsilon_h(-p') - \varepsilon_h(-p') + i0} \quad (16)$$

is a Cooper loop in the material (a product of the two Green functions in the Cooper channel), $n_h^F(\varepsilon)$ is the Fermi-Dirac distribution function for heavy particles, and analogously for the full T -matrices T_{hl} , T_{lh} and T_{ll} and the Cooper loops K_{lh} , K_{lh} and K_{ll} .

If we expand the T -matrix for the heavy particles in the first two orders in the gas parameter, then according to Galitskii¹⁵ we get

$$T_{hh}(\Omega, \mathbf{p}) = \frac{4\pi a_h}{m_h} + \left(\frac{4\pi a_h}{m_h} \right)^2 (K_{hh} - K_{hh}^{\text{vac}}) + o\left[\left(\frac{4\pi a_h}{m_h} \right)^3 (K_{hh} - K_{hh}^{\text{vac}})^2 \right], \quad (17)$$

where

$$\frac{4\pi a_h}{m_h} \approx \frac{U_{hh}d^3}{1 - U_{hh}d^3 K_{hh}^{\text{vac}}} \quad (18)$$

and coincides with Kanamori approximation for the vacuum T -matrix,

$$K_{hh}^{\text{vac}}(\Omega, \mathbf{p}) = \int \frac{d^3 \mathbf{p}' / (2\pi)^3}{\Omega - \frac{(\mathbf{p}' + \mathbf{p})^2}{2m_h} - \frac{p'^2}{2m_h}}$$

is the Cooper loop in vacuum (rigorously speaking the scattering length is defined via $K_{hh}^{\text{vac}}(0,0)$ but the difference between $K_{hh}^{\text{vac}}(\Omega, \mathbf{p})$ and $K_{hh}^{\text{vac}}(0,0)$ is proportional to the gas-parameter $a_h p_{Fh}$ and is small). K_{hh} in Eq. (17) is the full

Cooper loop (cooperon) in heavy particles given by Eq. (16). For low densities and energies close to ε_F we can show that the terms which we neglect in T_{hh} are small relative to the gas parameter

$$\frac{4\pi a_h}{m_h} (K_{hh} - K_{hh}^{\text{vac}}) \sim a_h p_{Fh}.$$

The self-energy of the heavy particles Σ_{hh} to second order in the gas-parameter is given by

$$\begin{aligned} \Sigma_{hh}(p) &= \sum_k T_{hh}(k+p) G_h(k) \approx \frac{4\pi a_h}{m_h} \sum_k G_h(k) \\ &- \left(\frac{4\pi a_h}{m_h} \right)^2 \sum_k (K_{hh} - K_{hh}^{\text{vac}}) G_h(k) + o(a_h p_{Fh})^3. \end{aligned} \quad (19)$$

The first term turns out to be $(4\pi a_h / m_h) n_h$. It is just the Hartree-Fock contribution. For the second term we can make an analytic continuation $i\omega_n \rightarrow \omega + i0$ for the boson propagator K_{hh} and the fermion propagator G_h . As a result (noting that $\text{Im } K_{hh}^{\text{vac}} = 0$), for the imaginary part of $\Sigma_{hh}^{(2)}$, we get

$$\begin{aligned} \text{Im } \Sigma_{hh}^{(2)}(\varepsilon, \mathbf{p}) &\approx \left(\frac{4\pi a_h}{m_h} \right)^2 \sum_{\mathbf{k}} \text{Im } K_{hh}(\varepsilon_k + \varepsilon, \mathbf{k} + \mathbf{p}) \\ &\times [n_B(\varepsilon_k + \varepsilon) + n_F(\varepsilon_k)] = - \left(\frac{4\pi a_h}{m_h} \right)^2 \\ &\times \pi \int \frac{d^3 \mathbf{k}}{(2\pi)^3} \int \frac{d^3 \mathbf{p}'}{(2\pi)^3} [1 - n_h^F(\mathbf{p}' + \mathbf{p} \\ &+ \mathbf{k}) - n_h^F(-\mathbf{p}')] [n_B(\varepsilon_k + \varepsilon) + n_F(\varepsilon_k)] \\ &\times \delta(\varepsilon + \varepsilon_h(\mathbf{k}) - \varepsilon_h(\mathbf{p}' + \mathbf{p} + \mathbf{k}) \\ &- \varepsilon_h(-\mathbf{p}')) \end{aligned} \quad (20)$$

and, analogously, for the real part of $\Sigma_{hh}^{(2)}$, we have

$$\begin{aligned} \text{Re } \Sigma_{hh}^{(2)}(\varepsilon, \mathbf{p}) &= \left(\frac{4\pi a_h}{m_h} \right)^2 \sum_{\mathbf{k}} [\text{Re } K_{hh}(\varepsilon_k + \varepsilon, \mathbf{k} + \mathbf{p}) \\ &- \text{Re } K_{hh}^{\text{vac}}(\varepsilon_k + \varepsilon, \mathbf{k} + \mathbf{p})] \\ &\times [n_B(\varepsilon_k + \varepsilon) + n_F(\varepsilon_k)], \end{aligned} \quad (21)$$

where for the real part of the Cooper loop in vacuum

$$\text{Re } K_{hh}^{\text{vac}}(\varepsilon_k + \varepsilon, \mathbf{k} + \mathbf{p}) = \int \frac{d^3 \mathbf{p}'}{(2\pi)^3} P \frac{2m_h}{\mathbf{k}^2 + \mathbf{p}^2 - (\mathbf{p}' + \mathbf{k} + \mathbf{p})^2 - p'^2} \quad (22)$$

is calculated at the resonance $\Omega = \varepsilon_k + \varepsilon_p$ (or for $\varepsilon = \varepsilon_p$), and P denotes the principal value. In Eqs. (20) and (21)

$$n_B(\Omega) = \frac{1}{e^{\Omega/T} - 1} \quad \text{and} \quad n_F(\Omega) = \frac{1}{e^{\Omega/T} + 1}$$

are the Bose and Fermi distribution functions and, correspondingly,

$$n_B(\varepsilon_k + \varepsilon) + n_F(\varepsilon_k) = \frac{1}{2} \left[\text{cth} \frac{(\varepsilon_k + \varepsilon)}{2T} - \text{th} \frac{\varepsilon_k}{2T} \right]. \quad (23)$$

The real part of the Cooper-loop in matter made up of heavy particles is

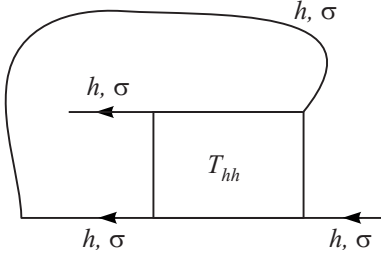


FIG. 4. An exchange-type diagram for the self-energy $\Sigma_{hh}^{\sigma\sigma}$ which contains the matrix element $a_{\sigma}^{+}a_{\sigma}^{+}a_{\sigma}a_{\sigma}$ and, thus, is absent in the Hubbard model.

Re $K_{hh}(\varepsilon_{\mathbf{k}} + \varepsilon, \mathbf{k} + \mathbf{p})$

$$= \int \frac{d^D \mathbf{p}'}{(2\pi)^3} \frac{1 - n_h^F(\mathbf{p}' + \mathbf{p} + \mathbf{k}) - n_h^F(-\mathbf{p}')}{\varepsilon + \varepsilon_h(\mathbf{k}) - \varepsilon_h(\mathbf{p}' + \mathbf{p} + \mathbf{k}) - \varepsilon_h(-\mathbf{p}')}$$

The analytic continuation for $\Sigma_{hh}^{(2)}$ in the 2D case is similar to the 3D case.

Note that for $\Omega/T \gg 1$ the Bose distribution function $n_B(\Omega) \rightarrow 0$ and the Fermi distribution function $n_F(\Omega) \rightarrow \theta(\Omega)$, a step-function. Hence, as $T \rightarrow 0$, $\text{Im} \Sigma_{hh}$ and $\text{Re} \Sigma_{hh}$ acquire the standard forms.^{15,16,18} In fact, for low temperatures $T \ll W_h \ll W_l$, the most convenient way is to evaluate $\text{Im} \Sigma_{hh}^{(2)}(\varepsilon)$ as $T \rightarrow 0$, thereby obtaining the standard Fermi-liquid result $\text{Im} \Sigma_{hh}^{(2)} \sim \varepsilon^2$ and then take the temperature average over the corresponding Fermi distribution function $n_F(\varepsilon)$. Thus, $\varepsilon \sim T$ over the lifetimes (or, as we show later, over the scattering times) of the quasiparticles. Evaluating Σ_{hl} , Σ_{lh} , and Σ_{ll} at low temperatures in the first two orders in the gas-parameter is similar to the evaluating Σ_{hh} in both the 3D and 2D cases.

At higher temperatures, however, we should note that $n_B(\Omega) \rightarrow T/\Omega$ for $T \gg \Omega$. The Fermi distribution function is “washed” out at these temperatures. Accordingly $n_B(\Omega) = \frac{1}{2}(1 - \Omega/2T)$. These approximations are important for calculating $\text{Im} \Sigma$ at higher temperatures $T > W_h$.²²

Note that, in contrast with the model of a slightly non-ideal Fermi gas,^{15,16,18} the Hubbard model does not contain an exchange-type diagram for Σ_{hh} (Fig. 4) since the T -matrix in this diagram corresponds to incoming and outgoing heavy particles with the same spin-projection $a_{\sigma}^{+}a_{\sigma}^{+}a_{\sigma}a_{\sigma}$ while the Hubbard model contains only the matrix elements $a_{\uparrow}^{+}a_{\downarrow}^{+}a_{\downarrow}a_{\uparrow}$.

Note also that when we expand the T -matrix to second order in the gas parameter, we implicitly assume that the T -matrix itself does not have a simple pole-structure of the type typical of a boson propagator. This is a case for partially filled band, i.e., $n_h d^D \ll 1$, and a low energy sector where $0 < \varepsilon < W_h \ll U_{hh}$. We effectively neglect the lattice in this expansion.

Including the lattice, however, produces two poles for the full (unexpanded) T -matrix of the heavy particles in (15). The first is related to the so-called antibound state predicted by Anderson²⁰ and corresponds to large positive energy $\varepsilon \sim U_{hh}$. The second pole, found by Engelbrecht and Randeria,²¹ corresponds to a negative energy and, in 2D, yields

$$\varepsilon = -2\varepsilon_{Fh} - \frac{2\varepsilon_{Fh}^2}{W_h} (1 - 2n_h) \left(1 - \frac{W_h}{U_{hh}} \right). \quad (24)$$

It describes the bound state of two holes below the bottom of the heavy band ($\varepsilon < -2\varepsilon_{Fh}$). Thus, it has a zero imaginary part and does not contribute to $\text{Im} T$. (This mode produces non-analytical corrections to $\text{Re} \Sigma_{hh} \sim |\varepsilon|^{5/2}$ in 2D). We can neglect both these contributions to the self-energy when calculating the effective masses and lifetimes below. A more rigorous approach to the generalization of Galitskii’s results for the self-energy¹⁵ to the case of finite temperatures (which is important for kinetic applications) will be discussed in a later paper.

V. ELECTRON-POLARON EFFECT AND OTHER MECHANISMS FOR HEAVY MASS-ENHANCEMENT. THE TENDENCY TOWARDS PHASE-SEPARATION

The Green-functions for heavy and light electrons for $T \rightarrow 0$ are

$$\begin{aligned} G_h(\omega, \mathbf{q}) &= \frac{1}{\omega - \varepsilon_h(q) - \Sigma_h(\omega, \mathbf{q})} \\ &\approx \frac{Z_h}{\omega - \varepsilon_h^*(q) + i0}; \text{ and analogously } G_l(\omega, \mathbf{q}) \\ &\approx \frac{Z_l}{\omega - \varepsilon_l^* + i0}, \end{aligned} \quad (25)$$

where

$$\varepsilon_h^*(q) = \frac{q^2 - p_{Fh}^2}{2m_h^*} \quad \text{and} \quad \varepsilon_l^*(q) = \frac{q^2 - p_{Fl}^2}{2m_l^*} \quad (26)$$

are renormalized quasiparticle spectra, and

$$\begin{aligned} Z_h^{-1} &= \left(1 - \left. \frac{\partial \text{Re} \Sigma_h^{(2)}(\omega, \mathbf{q})}{\partial \omega} \right|_{\substack{\omega \rightarrow 0 \\ q \rightarrow p_{Fh}}} \right); \\ Z_l^{-1} &= \left(1 - \left. \frac{\partial \text{Re} \Sigma_l^{(2)}(\omega, \mathbf{q})}{\partial \omega} \right|_{\substack{\omega \rightarrow 0 \\ q \rightarrow p_{Fl}}} \right) \end{aligned} \quad (27)$$

are the Z -factors for heavy and light electrons. Substituting the leading contribution from $\text{Re} \Sigma_{hl}^{(2)}(\omega, \mathbf{q})$ to $\text{Re} \Sigma_h^{(2)}(\omega, \mathbf{q})$ in Eq. (27) yields

$$\begin{aligned} \lim_{\omega \rightarrow 0} \frac{\partial \text{Re} \Sigma_{hl}^{(2)}(\omega, \mathbf{q})}{\partial \omega} &\sim - \left(\frac{4\pi a_{hl}}{m_{hl}^*} \right)^2 \int \int \frac{d^D \mathbf{p}}{(2\pi)^D} \frac{d^D \mathbf{p}'}{(2\pi)^D} \\ &\times \frac{[1 - n_h^F(\mathbf{p}' + \mathbf{p}) - n_h^F(-\mathbf{p}')] n_l^F(\mathbf{p} - \mathbf{q})}{[\varepsilon_l(\mathbf{p} - \mathbf{q}) - \varepsilon_l(\mathbf{p}' + \mathbf{p}) - \varepsilon_h(-\mathbf{p}')]^2}, \end{aligned} \quad (28)$$

where $n_B(\Omega) \rightarrow 0$ and $n_F(\Omega)$ is a step-function for $\Omega/T \gg 1$; $a_{hl} \approx d$ is related to the vacuum T -matrix T_{hl} ; and, $m_{hl} \approx ml$. Replacing

$$\frac{d^D \mathbf{p}}{(2\pi)^D} \frac{d^D \mathbf{p}'}{(2\pi)^D}$$

by $N_l^2(0) d\varepsilon_l(\mathbf{p}) d\varepsilon_l(\mathbf{p}')$ in Eq. (28) (where $N_l(0)$ is the density of states for light particles), and noting that $\varepsilon_L(\mathbf{p} - \mathbf{q}) < 0$, while $\varepsilon_L(\mathbf{p}' + \mathbf{p}) > 0$, we can easily check that for $m_h \gg m_l$ (or equivalently for $\varepsilon_{Fl} \gg \varepsilon_{Fh}$) this expression contains a large logarithm. Thus the Z -factor for the heavy particles becomes

$$Z_h^{-1} \approx 1 + 2f_0^2 \ln \frac{m_h}{m_l}, \quad (29)$$

where $f_0 = 2p_{F_l}d/\pi$ is the gas parameter in 3D and, equivalently, $f_0 = 1/[2 \ln(1/p_{F_l}d)]$ in 2D. Note that the contribution to Z_h from $\text{Re} \Sigma_{hh}^{(2)}$ does not contain a large logarithm. Thus, for the effective mass of a heavy particle in Eq. (25)^{16,18} we obtain

$$\frac{m_h^*}{m_h} = Z_h \left(1 + \left. \frac{\partial \text{Re} \Sigma_{hl}^{(2)}(\varepsilon_h(\mathbf{q}), \mathbf{q})}{\partial \varepsilon_h(\mathbf{q})} \right|_{\varepsilon_h(q) \rightarrow 0} \right). \quad (30)$$

Thus, as usual, the Z -factor enhances the heavy-mass, with

$$\frac{m_h^*}{m_h} \sim Z_h^{-1} \sim \left(1 + 2f_0^2 \ln \frac{m_h}{m_l} \right). \quad (31)$$

The analogous calculations for Z_l with $\text{Re} \Sigma_{lh}$ and $\text{Re} \Sigma_{ll}$ yields only $m_l^*/m_l \sim Z_l^{-1} \sim (1+f_0^2)$. If the parameter $2f_0^2 \ln(m_h/m_l) > 1$, then we are in the situation of strong electron-polaron effect. In this range of parameters, to get a correct polaron exponent diagrammatically, we should sum up the so-called maximally crossed diagrams for $\text{Re} \Sigma_{hl}$. The exponent could be evaluated, however, by a different technique based on the non-adiabatic part of the many-particle wave-function¹ for a heavy particle dressed in a cloud of electron-hole pairs of light particles. This yields

$$\frac{m_h^*}{m_h} \sim Z_h^{-1} = \left(\frac{m_h}{m_l} \right)^{b/1-b}, \quad (32)$$

where $b = 2f_0^2$. When $b = \frac{1}{2}$ or equivalently for $f_0 = \frac{1}{2}$ (as for the coupling constant of the screened Coulomb interaction in the RPA scheme), we are in the so-called unitary limit. In this limit¹ the polaron exponent is

$$\frac{b}{1-b} = 1, \quad (33)$$

so that

$$\frac{m_h^*}{m_h} = \frac{m_h}{m_l}, \quad (34)$$

or equivalently

$$\frac{m_h^*}{m_l} = \left(\frac{m_h}{m_l} \right)^2. \quad (35)$$

Hence, starting with a ratio of the bare masses $m_h/m_l \sim 10$ (obtained, for instance, in the LDA approximation), we end up in the unitary limit with $m_h^*/m_l \sim 100$ (due to many-body EPE); this is a typical value of this ratio for uranium-based heavy-fermion (HF) systems.

Note that rigorously speaking (see Eq. (30)) the momentum dependence of $\text{Re} \Sigma_{hl}^{(2)}(\varepsilon_h(\mathbf{q}), \mathbf{q})$ is also very important for the evaluation of the effective mass. Very preliminary estimates by N. V. Prokof'ev and the author²³ show that in the zeroth approximation in m_l/m_h for the 3D case close to the Fermi-surface (for $\varepsilon_h(q) = q^2 - p_{F_h}^2/2m_h \rightarrow 0$ and $q \rightarrow p_{F_h}$)

$$\text{Re} \Sigma_{hl}^{(2)}(\varepsilon_h(\mathbf{q}), \mathbf{q}) \approx 2 \left(\frac{4\pi a_{hl}}{m_l} \right)^2 \int \frac{d^3 \mathbf{p}}{(2\pi)^3} \pi_{ll}(0, \mathbf{p}) n_h^F(\mathbf{p} - \mathbf{q}), \quad (36)$$

where

$$\Pi_{ll}(0, \mathbf{p}) = \int \frac{d^3 \mathbf{p}'}{(2\pi)^3} \frac{n_l^F(\varepsilon_{p'+p}) - n_l^F(\varepsilon_{p'})}{\varepsilon_l(\mathbf{p}') - \varepsilon_l(\mathbf{p}' + \mathbf{p})}, \quad (37)$$

is the static polarization operator for light particles. Given that $|\mathbf{p} - \mathbf{q}| < p_{F_h}$ and taking $q \approx p_{F_h}$ in Eq. (36), we can see that $\mathbf{p} \rightarrow 0$ and, using the asymptotic form for $\Pi_{ll}(0, \mathbf{p})$ for small $p \ll p_{F_l}$ (if the densities of heavy and light bands are not very different and $p_{F_l} \sim p_{F_h}$), we have

$$\lim_{p > 0} \Pi_{ll}(0, \mathbf{p}) = N_l(0) \left[1 - \frac{p^2}{12p_{F_l}^2} \right], \quad (38)$$

where $N_l(0) = m_l p_{F_l} / 2\pi^2$ is the 3D density of states for light electrons. Substituting $\lim_{p \rightarrow 0} \Pi_{ll}(0, \mathbf{p})$ from Eq. (38) in Eq. (36) yields

$$\text{Re} \Sigma_{hl}^{(2)}(\varepsilon_h(\mathbf{q}), \mathbf{q}) \approx \text{Re} \Sigma_{hl}^{(2)}(0, p_{F_h}) - \frac{q^2 - p_{F_h}^2 f_0^2 m_h n_h}{2m_h \cdot 9 m_l n_l}, \quad (39)$$

where $f_0 = 2dp_{F_l}/\pi$ is the 3D gas parameter, and $n_h = p_{F_h}^3/3\pi^2$ and $n_l = p_{F_l}^3/3\pi^2$ are the densities in the heavy and light bands.

The first term in Eq. (39) gives $\text{Re} \Sigma_{hl}^{(2)}(\varepsilon_h(\mathbf{q}), \mathbf{q})$ on the Fermi-surface (for $\varepsilon_h(q) = 0$ and $q = p_{F_h}$)

$$\text{Re} \Sigma_{hl}^{(2)}(0, p_{F_h}) \sim \frac{4f_0^2 n_h}{3 n_l} \varepsilon_{F_l} \left(1 - \frac{2 p_{F_h}^2}{15 p_{F_l}^2} \right) > 0 \quad (40)$$

when $p_{F_h} \sim p_{F_l}$.

This is a renormalization of the effective chemical potential of the heavy band to the second order of the gas parameter owing to the interaction of light and heavy particles.

Note that^{15,16} the renormalized heavy particle spectrum is

$$\begin{aligned} \varepsilon_h^*(q) &= \left(\frac{q^2}{2m_h} - \mu_h^{\text{eff}} \right) + \frac{2\pi}{m_l} n_l(\mu) a_{hl} + \text{Re} \Sigma_{hl}^{(2)}(\varepsilon_h(\mathbf{q}), \mathbf{q}) \\ &= \frac{q^2 - p_{F_h}^2}{2m_h^*}, \end{aligned} \quad (41)$$

where the scattering length $a_{hl} \approx d$, the effective chemical potential $\mu_h^{\text{eff}} = \mu_h + W_h/2 + \varepsilon_0$ is reckoned from the bottom of the heavy band, and the Hartree-Fock term $(2\pi/m_l)n_l(\mu)a_{hl}$ represents the first-order contribution in terms of the gas parameter to the self-energy $\text{Re} \Sigma_{hl}^{(1)}$. Thus, upon collecting the terms proportional to $\varepsilon_h(q) = q^2 - p_{F_h}^2/2m_h$, Eq. (41) yields

$$\frac{q^2 - p_{F_h}^2}{2m_h^*} = \varepsilon_h(q) \left[1 - \frac{f_0^2 m_h n_h}{9 m_l n_l} \right]. \quad (42)$$

Correspondingly, the effective mass of a heavy particle is given by

$$\frac{m_h^*}{m_h} = 1 + \left. \frac{\partial \operatorname{Re} \Sigma_{hl}^{(2)}(\varepsilon_h(q), \mathbf{q})}{\partial \varepsilon_h(q)} \right|_{\varepsilon_h \rightarrow 0} = \left(1 - \frac{f_0^2 m_h n_h}{9 m_l n_l} \right). \quad (43)$$

As a result, we get a much more dramatic enhancement of m_h^* than with EPE, which yields only $m_h/m_h^* \approx 1 - 2f_0^2 \ln(m_h/m_l)$ through the heavy particle Z-factor. Note that the contribution to m_h^*/m_h from $\operatorname{Re} \Sigma_{hh}^{(2)}(\varepsilon_h(q), \mathbf{q})$ owing to the ‘‘heavy-heavy’’ interaction is small compared to the contribution to m_h^* from $\operatorname{Re} \Sigma_{hl}^{(2)}$ (which is related to ‘‘heavy-light’’ interactions) because of the smallness of the ratio of the bare masses, i.e., $m_l/m_h \ll 1$. Now we can collect the terms which do not depend upon $\varepsilon_h(q)$ in Eq. (41). Thus, for the effective chemical potential of heavy electrons we get

$$\mu_h^{\text{eff}} = \frac{p_{Fh}^2}{2m_h} + \frac{2\pi}{m_l} n_l(\mu) a_{hl} + \operatorname{Re} \Sigma_{hl}^{(2)}(0, p_{Fh}). \quad (44)$$

Note that the contributions to μ_h^{eff} from the heavy-electron Hartree–Fock term ($2\pi/m_h n_h(\mu) a_{hh}$ and from $\operatorname{Re} \Sigma_{hh}^{(2)}(0, p_{Fh})$ (which is related to ‘‘heavy-heavy’’ interactions) are small compared to the ‘‘heavy-light’’ contributions because of the smallness of the ratio of the bare masses, $m_l/m_h \ll 1$.

The 2D static polarization operator is

$$\Pi_{ll}(0, \mathbf{p}) = \frac{m_l}{2\pi} \left[1 - \operatorname{Re} \sqrt{1 - \frac{4p_{Fl}^2}{p^2}} \right]$$

so that, for $p < 2p_{Fl}$, $\Pi_{ll}(0, \mathbf{p}) = m_l/(2\pi)$, is independent of p^2 , in contrast to the 3D case. Thus in 2D, EPE is the dominant mechanism for heavy mass enhancement.

A more accurate determination of the momentum dependence of $\operatorname{Re} \Sigma_{hl}^{(2)}(\varepsilon_h(q), \mathbf{q})$ for higher densities in the bands, together with the sum of the higher order contributions to $\operatorname{Re} \Sigma_{hl}$, will be the subject of a separate study.

Note that for the light particles, the momentum dependences of $\operatorname{Re} \Sigma_{lh}^{(2)}$ and $\operatorname{Re} \Sigma_{ll}^{(2)}$ yield only $m_l^*/m_l \sim 1 + f_0^2$, so that the light mass is not strongly enhanced in either 3D or 2D.

Note also that, with higher densities of the heavy band $n_h \sim n_c \leq 1$ (and a large difference in the densities of the bands, i.e., $n_l \ll 1$, so that $n_{\text{tot}} = n_h + n_l \leq 1$) other mechanisms for heavy-mass enhancement become more effective. That is, with these densities and large mismatches between n_h and n_l , there should be a tendency towards phase-separation in a two-band model.¹⁰

Note that, if we analyze the effective chemical potential of the heavy band (44) in the limit of a high density mismatch $n_h \gg n_l$ in 3D and evaluate the partial compressibility (square of the speed of sound for heavy particles),

$$k_{hh}^{-1} \sim c_h^2 = \frac{n_h}{m_h} \left(\frac{\partial \mu_h}{\partial n_h} \right)$$

we can already see the tendency towards phase-separation (towards negative compressibility) in the strong coupling limit and at low densities for $f_0^2 m_h p_{Fh} / m_l p_{Fl} \gg 1$, in qualitative agreement with Ref. 10. A more careful analysis of all the partial compressibilities in the system for larger f_0 and large mismatches between the densities will be the subject of a separate study.

In concluding this section we would like to emphasize that the physics of EPE and the determination of Z_h (in Ref. 1) are, to some extent, related to the well-known results of Nozieres *et al.*,²⁴ on infrared divergences in the description of the Brownian motion of heavy particles in a Fermi liquid and on the infrared divergences in the problem of x-ray photoemission from deep electron levels, as well as with the famous results of Anderson²⁵ on the orthogonality catastrophe for a 1D chain of N electrons with the addition of one impurity to the system.

Finally, we would like to mention here a competing mechanism that Fulde *et al.*,²⁶ first developed to explain the effective mass in praseodymium (Pr) and in some uranium-based molecules such as $\text{U}(\text{C}_8\text{H}_8)_2$. Fulde *et al.*, later generalized this mechanism to some other uranium-based HF compounds with localized and delocalized orbitals. This mechanism has a quantum chemical nature and is based on the scattering of conduction electrons on localized orbitals as in two-level systems. Here the mass-enhancement is governed by nondiagonal matrix elements of the Coulomb interaction that are not contained in the simple version of a two-band model (1). In this context we would also like to mention Ref. 27 which deals with mass-enhancement of conduction electrons owing to their being scattering on local f-levels split by the crystal field. dHvA experiments,²⁸ together with ARPES experiments²⁹ and thermodynamic measurements,³⁰ are the main instruments for reconstructing the Fermi-surface of HF compounds and for determining the effective mass (thus testing the predictions of various theories on mass-enhancement in uranium-based HF compounds).

VI. IMAGINARY PARTS OF THE SELF-ENERGIES IN THE HOMOGENEOUS STATE

As $T \rightarrow 0$ all the imaginary parts of the self-energies in the homogeneous state behave in a standard FL manner for equal densities of heavy and light electrons. For $\varepsilon_q > 0$ they are given by

$$\begin{aligned} \operatorname{Im} \Sigma_{hh}^{(2)}(\varepsilon_h(\mathbf{q}), \mathbf{q}) &= f_0^2 \frac{\varepsilon_h^2(\mathbf{q})}{\varepsilon_{Fh}}; \\ \operatorname{Im} \Sigma_{ll}^{(2)}(\varepsilon_l(\mathbf{q}), \mathbf{q}) &= f_0^2 \frac{\varepsilon_l^2(\mathbf{q})}{\varepsilon_{Fl}}. \end{aligned} \quad (45)$$

Thus, for Σ_{hl} and Σ_{lh} we have

$$\begin{aligned} \operatorname{Im} \Sigma_{hl}^{(2)}(\varepsilon_h(\mathbf{q}), \mathbf{q}) &= f_0^2 \frac{\varepsilon_h^2(\mathbf{q})}{\varepsilon_{Fh}}; \\ \operatorname{Im} \Sigma_{lh}^{(2)}(\varepsilon_l(\mathbf{q}), \mathbf{q}) &= f_0^2 \frac{\varepsilon_l^2(\mathbf{q}) m_h}{\varepsilon_{Fh} m_l}. \end{aligned} \quad (46)$$

Note that $n_B(\Omega) \rightarrow 0$ and $n_F(\Omega) \rightarrow \theta(\Omega)$ for $\Omega/T \gg 1$ in the general expression for $\operatorname{Im} \Sigma$ obtained in section IV.

VII. SCATTERING TIMES AND DRUDE CONDUCTIVITIES

For the inverse scattering times (more rigorously for the lifetimes) of the heavy and light particles when $\varepsilon \sim T$ we have

$$1/\tau_h = (1/\tau_{hh} + 1/\tau_{hl}) = f_0^2(T^2/\varepsilon_{Fh}). \quad (47)$$

Analogously, for light particles

$$1/\tau_l = (1/\tau_{ll} + 1/\tau_{lh}) \approx 1/\tau_{lh} \approx f_0^2 \frac{T^2 m_h}{\varepsilon_{Fh} m_l} > 1/\tau_h. \quad (48)$$

Now we can calculate the Drude conductivities according to the standard formula $\sigma = ne^2\tau/m$. For light electrons

$$\sigma_l = \frac{n_l e^2 \tau_l}{m_l} = \frac{n_l e^2 \varepsilon_{Fh} m_l}{f_0^2 T^2 m_h m_l} \sim \frac{n_l e^2}{f_0^2 p_{Fh}^2} \left(\frac{\varepsilon_{Fh}}{T} \right)^2. \quad (49)$$

Introducing the minimum Mott–Regel conductivities,

$$\sigma_{\min} = (e^2/\hbar)p_F \text{ in 3D and } \sigma_{\min} = e^2/\hbar \text{ in 2D,} \quad (50)$$

and using units with $\hbar=1$, for equal densities of heavy and light bands, i.e., $n_l = n_h$, we obtain

$$\sigma_l = \frac{\sigma_{\min}}{f_0^2} \left(\frac{\varepsilon_{Fh}}{T} \right)^2. \quad (51)$$

Analogously for σ_h , we have

$$\sigma_h = \frac{n_h e^2 \tau_h}{m_h} = \frac{n_h e^2 \varepsilon_{Fh}}{m_h f_0^2 T^2} \sim \frac{n_h e^2}{p_{Fh}^2} \left(\frac{\varepsilon_{Fh}}{T} \right)^2 \frac{1}{f_0^2}. \quad (52)$$

Thus the scattering times for heavy and light particles $1/\tau_h$ and $1/\tau_l$ differ, but the conductivities $\sigma \propto \tau/m$ are of the same order of magnitude:¹

$$\sigma_h \sim \frac{\sigma_{\min}}{f_0^2} \left(\frac{\varepsilon_{Fh}}{T} \right)^2 \sim \sigma_l. \quad (53)$$

The total conductivity is

$$\sigma = \sigma_h + \sigma_l \sim \frac{\sigma_{\min}}{f_0^2} \left(\frac{\varepsilon_{Fh}}{T} \right)^2 \quad (54)$$

so that the resistivity

$$R = \frac{1}{\sigma} = \frac{f_0^2}{\sigma_{\min}} \left(\frac{T}{\varepsilon_{Fh}} \right)^2 \quad (55)$$

behaves as in a Fermi-liquid, with $R(T) \propto T^2$ at low temperatures.

VIII. THE DIFFERENCE BETWEEN LIFETIMES AND TRANSPORT TIMES

Strictly speaking we calculate lifetimes and not transport times. However an exact solution of the coupled kinetic equations³¹ for heavy and light electrons including umklapp processes for not-too-low densities of the bands shows that, if $m_h \gg m_l$ and $p_{Fh} \sim p_{Fl} \sim p_F \leq 1/d$ then for all the times including τ_{lh} , τ_{hl} we get²²

$$\tau_{\text{transp}} = \tau_{\text{life-time}}. \quad (56)$$

Umklapp processes for the interaction of heavy and light electrons imply that

$$\mathbf{p}_{1h} + \mathbf{p}_{2l} = \mathbf{p}_{3h} + \mathbf{p}_{4l} + \mathbf{K}, \quad (57)$$

where $K \sim \pi/d$ is the wave-vector of the reciprocal lattice. For $p_{Fh} \sim p_{Fl}$ this means that the densities in the light and heavy bands cannot be very small (otherwise the resistivity will be exponentially small). Hence to the accuracy of our estimates,

$$R \sim \frac{f_0^2}{\sigma_{\min}} \left(\frac{T}{W_h} \right)^2 \quad (58)$$

and in all the estimates for inverse scattering times and conductivities we can replace ε_{Fh} with W_h and ε_{Fl} with W_l . Moreover for $m_h^*/m_h \gg 1$ we can replace m_h with m_h^* (or equivalently W_h with W_h^*), so that the final result for the resistivity is

$$R \sim \frac{f_0^2}{\sigma_{\min}} \left(\frac{T}{W_h^*} \right)^2. \quad (59)$$

IX. THE CHEMICAL POTENTIAL AT HIGHER TEMPERATURES $T > W_h^*$

If $T > W_h^*$ the heavy band is totally destroyed (more precisely, it is destroyed for $f_0^2 T = W_h^*$, as we shall see soon). To be accurate let us first calculate the effective chemical potential $\mu_h^{\text{eff}} = \mu + W_h/2 + \varepsilon_0$ in Eq. (3) in this situation.

Generally speaking $n_h + n_l = n_{\text{tot}} = \text{const}$ and only the total density is conserved. However, in our case for a large difference between the bare masses, with $m_h \gg m_l$, the density of each band is essentially conserved independently, i.e., $n_h \approx \text{const}$ and $n_l \approx \text{const}$. For heavy particles, all the states in a band will be uniformly populated at these temperatures. For $T > W_h$ (assuming $m_h^*/m_h \sim 1$) the effective chemical potential of the heavy particles is

$$\mu_h^{\text{eff}} = \mu + \frac{W_h}{2} + \varepsilon_0 \sim T \ln \left(\frac{1}{n_h d^D} \right). \quad (60)$$

Thus we have Boltzmann behavior for μ_h^{eff} . The Fermi-Dirac distribution function for the heavy particles is

$$\begin{aligned} n_h(\varepsilon) &= (e^{p^2/2m_h - \mu_h^{\text{eff}}/T} + 1)^{-1} = \left[\left(1 + \frac{p^2}{2m_h T} \right) e^{-\mu_h^{\text{eff}}/T} \right. \\ &\quad \left. + 1 \right]^{-1} \\ &\approx e^{\mu_h^{\text{eff}}/T} \left(1 + \frac{p^2}{2m_h T} \right)^{-1} \approx e^{\mu_h^{\text{eff}}/T} = \text{const}. \end{aligned} \quad (61)$$

For light particles, because $m_h \gg m_l$, at temperatures $W_h \ll T \ll W_l$ the effective chemical potential will be approximately the same as at $T=0$. Indeed for $\mu_{\text{eff}}^l = \mu + W_l/2$, we get

$$\begin{aligned} n_l(\varepsilon) &= (e^{p^2/2m_l - \mu_{\text{eff}}^l/T} + 1)^{-1} \approx (e^{(p^2 - p_{Fl}^2)/2m_l T} + 1)^{-1} \\ &\approx \theta \left(\frac{p^2}{2m_l} - \varepsilon_{Fl} \right) \quad \text{for } T \ll \varepsilon_{Fl} \end{aligned} \quad (62)$$

so that the effective chemical potential of the light particles is

$$\mu_{\text{eff}}^l \approx \varepsilon_{Fl}. \quad (63)$$

X. EVALUATING THE SCATTERING TIMES AT HIGHER TEMPERATURES $W_h^* < T < W_l$

For light particles the scattering time, given by $1/\tau_l = f_0^2 T^2 / W_l$, does not change. However,

$$\frac{1}{\tau_{lh}} = f_0^2 W_h \frac{m_h}{m_l} \quad (64)$$

implies almost elastic scattering of light electrons on heavy electrons, as if on immobile (static) impurities in zeroth order in W_h/W_l . Note that $W_h m_h = W_h^* m_h^*$.

For heavy electrons we should take the bosonic $n_B(\Omega) \approx T/\Omega$ and fermionic $n_F(\Omega) \approx \frac{1}{2}(1 - \Omega/2T)$ contributions to $\text{Im} \Sigma^{(2)}$ for $\Omega/T \ll 1$ and, therefore, to the scattering times. This yields

$$\frac{1}{\tau_{hh}} = f_0^2 W_h \quad (65)$$

for scattering of heavy electrons on each other when they uniformly occupy the heavy band and can only transfer an energy $\sim W_h$ to each other.¹ For $m_h^* \gg m_h$ we can replace W_h by W_h^* in Eq. (65). At the same time

$$\frac{1}{\tau_{hl}} = f_0^2 T \quad (66)$$

implies marginal Fermi-liquid behavior for diffusive motion of the heavy electrons surrounded by light electrons.

XI. 3D RESISTIVITY FOR $T > W_h^*$

For the scattering times of heavy and light particles when $T > W_h^*$ we, therefore, have

$$1/\tau_l = 1/\tau_{ll} + 1/\tau_{lh} \approx 1/\tau_{lh} = f_0^2 W_h \frac{m_h}{m_l} \quad (67)$$

($T^2/W_l < W_h m_h/m_l$ for $T < W_l$). Note that

$$f_0^2 W_h \frac{m_h}{m_l} = f_0^2 W_h^* \frac{m_h^*}{m_l} \sim f_0^2 W_l$$

in Eq. (67). At the same time,

$$1/\tau_h = 1/\tau_{hh} + 1/\tau_{hl} \approx 1/\tau_{hl} = f_0^2 T. \quad (68)$$

Thus, the heavy component is marginal while the light component is not.

For conductivity of the light band we have

$$\sigma_l = \frac{n_l e^2 \tau_l}{m_l} \approx \frac{m_l e^2 \tau_{lh}}{m_l} = \frac{\sigma_{\min}}{f_0^2}. \quad (69)$$

For the heavy band, the Drude formula should be modified since $\delta n_h / \delta T \sim W_h^* / T$ for $T > W_h^*$. Then we immediately obtain

$$\sigma_h = \frac{\sigma_{\min}}{f_0^2} \left(\frac{W_h^*}{T} \right)^2. \quad (70)$$

As a result, for the resistivity one arrives at

$$R = \frac{1}{\sigma_h + \sigma_l} = \frac{f_0^2}{\sigma_{\min}} \frac{(T/W_h^*)^2}{1 + (T/W_h^*)^2} = \frac{f_0^2}{\sigma_{\min}} \frac{1}{1 + (W_h^*/T)^2}. \quad (71)$$

For $T > W_h^*$ the resistivity $R \approx f_0^2 / \sigma_{\min}$ approaches saturation. We, therefore, obtain a residual resistivity at high temperatures owing to conductivity in a light band. This is a very nontrivial result

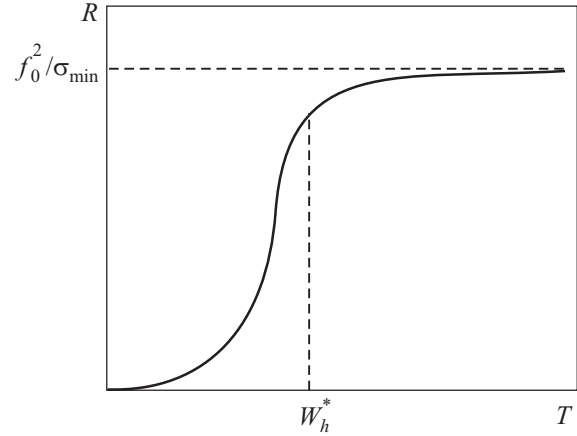


FIG. 5. The resistivity characteristics $R(T)$ in a the 3D two-band model.

XII. DISCUSSION OF THE RESISTIVITY AT HIGHER TEMPERATURES

When $W_h^* < 1/\tau_h$ or, equivalently $f_0^2 T > W_h^*$, coherent motion in the heavy band is totally destroyed. The heavy particles begin to move diffusively among the surrounding light particles. Strictly speaking, in this regime the diagram technique can be used only for light particles and not for heavy particles.

However, the exact solution for the density matrix equation obtained in Ref. 1 shows that $1/\tau_{hl}$ is qualitatively the same as in our estimates when $f_0^2 T > W_h^*$; the inverse scattering time, $1/\tau_{lh}$ is also qualitatively the same because of its physical meaning (scattering of light electrons on heavy ones such as immobile impurities). That is why σ_h , σ_l and hence $R(T)$ behave smoothly for $f_0^2 T \gg W_h^*$.

XIII. THE IDEA OF A HIDDEN HEAVY BAND FOR HTSC

The 3D resistivity characteristics $R(T)$ acquire a form (see Fig. 5) which is frequently observed in uranium-based HF (for example in UNi_2Al_3). $R(T)$ mimics a linear behavior between T^2 and const (where it approaches saturation as $T \gg W_h^*$) in a crossover region of intermediate temperatures $T \sim W_h^*$. The same holds for magnetoresistance in Kapitza's well-known experiments:

$$\frac{R(H) - R(0)}{R(H)} \sim \frac{(\Omega_c \tau)^2}{1 + (\Omega_c \tau)^2} \sim \begin{cases} (\Omega_c \tau)^2 & \text{for } \Omega_c \tau < 1, \\ \text{const} & \text{for } \Omega_c \tau > 1, \end{cases} \quad (72)$$

where Ω_c is the cyclotron frequency.

In the crossover region $\Omega_c \tau \sim 1$ the magnetoresistance seems to depend linearly on Ω_c .

Thus, we find that for $T > W_h^*$, the heavy electrons are marginal but the light electrons are not. A natural question arises: is it possible to make the light electrons marginal, as well, and thereby obtain resistivity characteristics of the type $R(T) \propto T$ for $T > W_h^*$ while $R(T) \propto T^2$ for $T < W_h^*$. Resistivity characteristics of this sort could serve as an alternative scenario for explaining the normal properties in HTSC materials if we assume the existence of a hidden heavy band with a bandwidth smaller than the superconducting critical temperature T_c , i.e., $W_h^* < T_c$ (see Fig. 6). Then to get $R(T) \propto T^2$ (FL

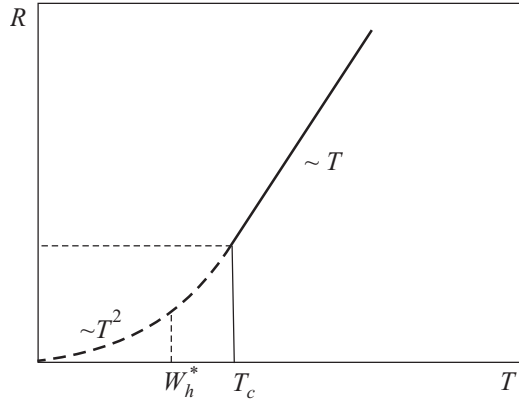


FIG. 6. The resistivity $R(T)$ in a superconducting material with a hidden heavy band for $W_h^* < T_c$ (W_h^* is an effective width of the heavy band).

behavior at low temperatures) we should suppress SC by applying a high magnetic field H down to low critical temperatures $T_c(H) < W_h^*$.

XIV. 2D WEAK-LOCALIZATION CORRECTIONS

The tendency towards marginalization of the light component shows up in the 2D case. We know that in 2D there are logarithmic corrections⁷ to the classical Drude formula for the conductivity owing to weak localization effects. But according to our ideology, heavy particles play the role of impurities for scattering of light particles. That is why the correct expression for the conductivity σ_l of the light band in the absence of spin-orbital coupling is

$$\sigma_l^{\text{loc}} = \frac{\sigma_{\text{min}}}{f_0^2} \left[1 - f_0^2 \ln \frac{\tau_\varphi}{\tau} \right], \quad (73)$$

where, according to 2D weak-localization theory, τ is the elastic collision time, while τ_φ is the inelastic collision (decoherence) time. In our case,

$$\tau = \tau_{ei} = \tau_{lh}, \quad \text{while } \tau_\varphi = \tau_{ee} = \tau_{ll}, \quad \text{and } \tau_{ll} \gg \tau_{lh}, \quad (74)$$

where τ_{ei} and τ_{ee} are the scattering times for electrons on impurities and other electrons, respectively. Thus, between two collisions of a light particle on another light particle, it undergoes many collisions with heavy particles (see Fig. 7).

As a result, the velocity of the light particle is greatly reduced (as is the diffusive motion) and two characteristic lengths appear in the theory: the elastic length,

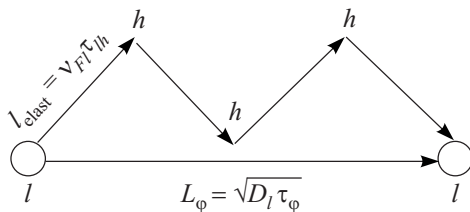


FIG. 7. Multiple scattering of light particle on heavy particles in between collisions of light particles on light particles. L_φ is the diffusive length, l_{elast} is the elastic length, D_l and v_{Fl} are the diffusion coefficient and Fermi velocity of the light electrons, and τ_{lh} and τ_φ are the elastic time for scattering of light electrons on heavy electrons and the inelastic (decoherence) time.

$$l_{\text{elast}} = v_{Fl} \tau_{lh} \quad (75)$$

and the diffusive length

$$L_\varphi = \sqrt{D_l \tau_\varphi} \quad (76)$$

where D_l is a diffusion coefficient for the light electrons and v_{Fl} is the Fermi velocity of the light electrons.

That is why, according to Altshuler-Aronov,⁷ in a more rigorous theory we should replace the inverse scattering time

$$\frac{1}{\tau_{ll}(\varepsilon)} \sim \int_0^\varepsilon d\omega \int_0^\omega d\varepsilon' \int_0^\infty \frac{a_{ll}^2}{m_l^2 (v_{Fl} q)^2} q dq = f_0^2 \frac{T^2}{W_l} \quad (77)$$

by

$$\frac{1}{\tilde{\tau}_{ll}(\varepsilon)} \sim \int_0^\varepsilon d\varepsilon' \int_0^\omega d\varepsilon'' \int_0^\infty \frac{a_{ll}^2}{m_l^2 (i\varepsilon' + D_l q^2)^2} q dq, \quad (78)$$

where the scattering length $a_{ll} \sim d$. In fact, we replace $v_{Fl} q$ with a ‘‘cooperon’’ pole ($i\varepsilon' + D_l q^2$) in the Altshuler-Aronov terminology. Thus, when evaluating $\tilde{\tau}_{ll}$, the characteristic wave-vectors $q \sim \sqrt{\varepsilon/D_l}$, where ε is an energy variable. The Altshuler-Aronov effect in 2D yields

$$\frac{1}{\tilde{\tau}_{ll}(\varepsilon)} = f_0^2 \frac{\varepsilon}{N_l(0) D_l}, \quad (79)$$

where $N_l(0) = m_l/2\pi$ is a 2D density of states for the light electrons. For the diffusion coefficient we can use the estimate

$$D_l = v_{Fl}^2 \tau_{lh} \quad (80)$$

so that, since the inverse scattering time $1/\tau_{lh}(\varepsilon) = f_0^2 W_h (m_h/m_l) \approx f_0^2 W_l$ according to Eq. (68), we obtain

$$\frac{1}{\tilde{\tau}_{ll}(\varepsilon)} \sim \frac{f_0^2 W_l}{(m_l/\pi) v_{Fl}^2} \varepsilon \sim f_0^4 \varepsilon. \quad (81)$$

Thus $1/\tilde{\tau}_{ll}$ also becomes marginal when $\varepsilon \sim T$. For the logarithmic corrections to conductivity we have

$$\frac{\tau_\varphi}{\tau} = \frac{\tilde{\tau}_{ll}}{\tau_{lh}} = \frac{W_l}{f_0^2 T} \gg 1 \quad (82)$$

so that

$$\sigma_l^{\text{loc}} = \frac{\sigma_{\text{min}}}{f_0^2} \left[1 - f_0^2 \ln \frac{W_l}{f_0^2 T} \right]. \quad (83)$$

For $f_0^2 T \sim W_h$, we have $\ln W_l/f_0^2 T \sim \ln W_l/W_h$ and

$$Z_h = \frac{\sigma_l^{\text{loc}}}{\sigma_l} = 1 - f_0^2 \ln \frac{W_l}{W_h}. \quad (84)$$

Thus, for $f_0^2 T \sim W_h$, the enhancement in the heavy particle Z-factor owing to EPE and the localization of light particles owing to the Altshuler-Aronov corrections are governed by the same parameter $f_0^2 \ln(m_h/m_l)$ in 2D.

XV. JUSTIFICATION OF THE EXPRESSION FOR 2D LOCALIZATION CORRECTIONS

In principle, impurities are mobile and have some recoil energy. That is why the formula $\sigma_l^{\text{loc}}/\sigma_l = 1 - f_0^2 \ln(W_l/f_0^2 T)$ must be justified (at least the temperature dependent factor under the logarithm should be T or T^α). To do this we need to

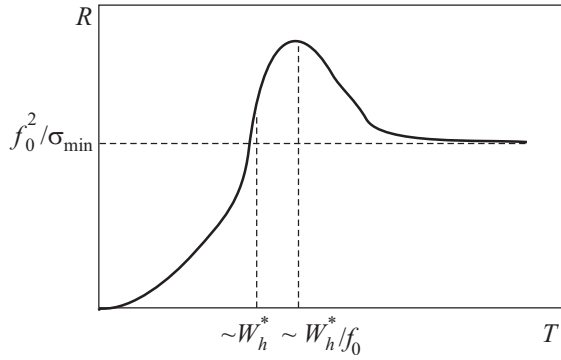


FIG. 8. The 2D resistivity $R(T)$ in a two-band model with one narrow band. It has a maximum and a localization tail at high temperatures $T > W_h^*$.

estimate the energy lost by a light particle before it collides with another light particle (i.e., the energy lost by a light particle between collisions with light particles). The number of collisions with heavy particles between light-light scattering events is $L_\varphi / l_{\text{elast}}$. The maximum energy loss in one collision is W_h^* . The total loss is

$$W_h^* \frac{L_\varphi}{l_{\text{elast}}} = W_h^* \sqrt{\frac{W_l}{T}}.$$

The energy of the light particle itself is T . This means that for $W_h^* \sqrt{W_l/T} < T$ or, equivalently, for

$$T > W_h^* \left(\frac{W_l}{f_0^2 W_h^*} \right)^{1/3}. \quad (85)$$

the energy loss is small and the heavy particles can be regarded as immobile impurities. Thus, the exponent α in the logarithm is 1.

XVI. THE 2D RESISTIVITY

The resistivity behaves qualitatively in 2D as follows:

$$R = \frac{f_0^2}{\sigma_{\text{min}}} \frac{1}{\left(\frac{W_h^*}{T} \right)^2 + \left(1 - f_0^2 \ln \frac{W_l}{f_0^2 T} \right)}. \quad (86)$$

It has a maximum for $T_{\text{max}} \sim W_h^* / f_0$ and a localization tail at higher temperatures (see Fig. 8). It is very interesting to determine the magnetoresistance in the 2D or layered case using a two-band model with one narrow band with a strong quantizing magnetic field H oriented perpendicular to the layers. Here we can expect a strong manifestation of the famous Aharonov-Bohm effect.³²

XVII. SUPERCONDUCTIVITY IN A TWO-BAND MODEL WITH ONE NARROW BAND

For the sake of completeness let us briefly consider the superconductivity problem using this type of model, namely a two-band Hubbard model with one narrow band. We concentrate on the 2D case where critical temperatures are already higher at low densities^{11,12} and consider the most typical case (see Fig. 1) $m_h > m_l$ and $p_{Fh} > p_{Fl}$ but we assume that the mismatch between the densities is still not large enough to cause phase separation. Note that in 2D, where only EPE is present, the restrictions on a homogeneous state

could milder than in 3D. At low densities $n_l d^2 < n_h d^2 \ll 1$ the maximum T_c corresponds to p -wave pairing^{11,12} and is governed by the enhanced Kohn–Luttinger mechanism for SC.¹³ The general expression for the effective interaction V_{eff} of the heavy particles (to the irreducible bare vertex for the Cooper channel) in the first two orders in the gas-parameter is^{11,12}

$$V_{\text{eff}}(\mathbf{p}_h, \mathbf{p}'_h) = T_{hh} + T_{hh}^2 \pi_{hh}(0, \tilde{\mathbf{q}}_h = \mathbf{p}_h + \mathbf{p}'_h) - 2T_{hl}^2 \Pi_{ll}(0, \mathbf{q}_h = \mathbf{p}_h - \mathbf{p}'_h), \quad (87)$$

where \mathbf{p} and \mathbf{p}' are the incoming and outgoing momenta for the heavy particles in the Cooper channel and $|\mathbf{p}_h| = |\mathbf{p}'_h| = p_{Fh}$, and

$$q_h^2 = 2p_{Fh}^2(1 - \cos \varphi); \quad \tilde{q}_h^2 = 2p_{Fh}^2(1 + \cos \varphi) \quad (88)$$

are the squares of the momentum transfer (for q_h^2) and transferred momentum with an account of crossing squared (for \tilde{q}_h^2). Note that in Eq. (88) both $q_h \leq 2p_{Fh}$ and $\tilde{q}_h \leq 2p_{Fh}$ for superconductivity. The second term in Eq. (87) is related to the exchange diagram^{11–13} for the heavy electrons and the third term, to the static polarization operator for the light electrons.^{11,12}

In Eq. (87) for Π_{hh} and Π_{ll} we have

$$\begin{aligned} \Pi_{hh}(0, \tilde{\mathbf{q}}_h) &= Z_h^2 \frac{m_h^*}{2\pi} \left[1 - \text{Re} \sqrt{1 - \frac{4p_{Fh}^2}{\tilde{q}_h^2}} \right], \\ \Pi_{ll}(0, \mathbf{q}_h) &= Z_l^2 \frac{m_l}{2\pi} \left[1 - \text{Re} \sqrt{1 - \frac{4p_{Fl}^2}{q_h^2}} \right], \end{aligned} \quad (89)$$

where Z_h and m_h^* are the heavy-particle Z -factor and effective mass, Z_l and m_l are light-particle Z -factor and effective mass, and p_{Fh} and p_{Fl} are Fermi-momenta for the heavy and light electrons. Given that $Z_l \sim m_l / m_l^* \sim (1 \sim f_0^2)$, we can set $Z_l \sim 1$ and $m_l \sim m_l$ in the following. Finally in Eq. (87) for $p_{Fh} > p_{Fl}$ the T -matrices are

$$\begin{aligned} T_{hh} &= \frac{4\pi}{m_h^*} \frac{1}{\ln[1/(p_{Fh}^2 d^2)]} > 0, \\ T_{hl} &= \frac{4\pi}{m_l} \frac{1}{\ln[1/(p_{Fh}^2 d^2)]} > 0. \end{aligned} \quad (90)$$

Given that $\tilde{q}_h \leq 2p_{Fh}$ we find that $\Pi_{hh}(0, \tilde{\mathbf{q}}_h) = Z_h^2 m_h^* / 2\pi$ does not depend on the momentum transfer at crossing \tilde{q}_h .

At the same time $\Pi_{ll}(0, \mathbf{q}_h)$ has a nontrivial dependence on q_h for $p_{Fh} > p_{Fl}$. We can say^{11,12} that a large 2D Kohn anomaly (connected with the square-root in the expression for Π_{ll} in Eq. (89)) becomes effective in the SC problem and we have pairing of heavy electrons through polarization of light electrons (see Fig. 9). Note that standard s -wave pairing is suppressed in a two-band Hubbard model by the short-range Hubbard repulsion, which yields $T_{hh} > 0$ in the first-order contribution to V_{eff} in Eq. (87).

According to the Landau–Thouless criterion, the maximum critical temperature in our model corresponds to p -wave pairing (to pairing with magnetic quantum number $m=1$ in 2D), i.e.,

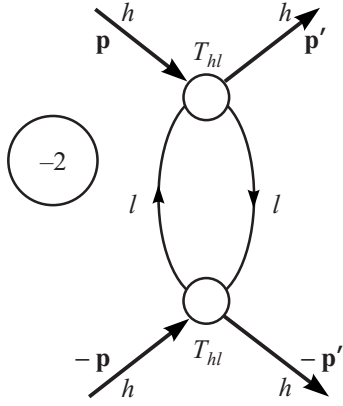


FIG. 9. The leading contribution to the effective interaction V_{eff} for p -wave pairing of heavy particles through polarization of light particles. The open circles represent the vacuum T -matrix T_{hl} .

$$-V_{\text{eff}}^{m=1} N_h^*(0) Z_h^2 \ln \frac{\varepsilon_{Fh}}{T_{c1}} = 1 \quad (91)$$

where $N_h^*(0) = m_h^*/2\pi$ is an effective 2D density of states for the heavy electrons; $\varepsilon_{Fh}^* = p_{Fh}^2/2m_h^*$ is the renormalized Fermi energy for the heavy electrons; and, $V_{\text{eff}}^{m=1}$ is a p -wave harmonic of the effective interaction. We thus have

$$V_{\text{eff}}^{m=1} = \int_0^{2\pi} V_{\text{eff}}(q \cos \varphi) \cos \varphi \frac{d\varphi}{2\pi}. \quad (92)$$

It has been shown^{11,12} that $V_{\text{eff}}^{m=1}$ depends on the relative populations of the two bands p_{Fh}/p_{Fl} and is given by

$$V_{\text{eff}}^{m=1} = N_l^*(0) \frac{p_{Fh}/p_{Fl} - 1}{p_{Fh}^2/p_{Fl}^2} T_{hl}^2(-2) < 0. \quad (93)$$

It also corresponds to attraction. $N_l^*(0) = m_l^*/2\pi$ is the 2D density of states for light electrons in Eq. (93). We can see that $V_{\text{eff}}^{m=1} \rightarrow 0$ as $p_{Fh}/p_{Fl} \rightarrow 1$ and $p_{Fh}/p_{Fl} \rightarrow \infty$. It is easy to show that $V_{\text{eff}}^{m=1}$ has a rather large and broad maximum¹² at $p_{Fh} = 2p_{Fl}$ or equivalently $n_h = 4n_l$. The maximum effective interaction is

$$V_{\text{eff}}^{m=1} = -\frac{1}{2} N_l^*(0) \left(\frac{4\pi}{m_l^* \ln(1/p_{Fh}^2 d^2)} \right)^2. \quad (94)$$

Correspondingly, the Landau–Thouless criterion for the superconducting temperature gives

$$\frac{m_h}{m_l} Z_h^2 2f_0^2 \ln \frac{\varepsilon_{Fh}}{T_{c1}} = 1 \quad (95)$$

where $f_0 = 1/\ln(1/p_{Fh}^2 d^2)$ is the 2D gas parameter. For $f_0^2 \ln(m_h/m_l) \leq 1$, EPE is weak and $m_h^* \approx m_h$. Thus $Z_h \approx 1$, $\varepsilon_{Fh}^* \approx \varepsilon_{Fh}$ and the Landau–Thouless criterion becomes $(m_h/m_l) 2f_0^2 \ln(\varepsilon_{Fh}/T_{c1}) = 1$. The effective gas-parameter in the formula for T_{c1} with weak EPE is $f_0(m_h/m_l)^{1/2}$. It is interesting that in the unitary limit $f_0 \rightarrow 1/2$, EPE yields an enhancement in m_h^* of

$$\frac{m_h^*}{m_l} Z_h^2 \sim \frac{m_h^*}{m_l} \frac{m_h^2}{(m_h^*)^2} \sim \frac{m_h^2}{m_l^2} \frac{m_l}{m_h^*} \sim 1. \quad (96)$$

Thus for the critical temperature in the unitary limit $f_0 \rightarrow 1/2$ we get

$$T_{c1} \sim \varepsilon_F^* e^{-1/(2f_0^2)} \sim \varepsilon_F^* e^{-2}. \quad (97)$$

This means that for $\varepsilon_{Fh}^* \sim 50$ K, already $T_{c1} \sim 5$ K at low densities, which is quite reasonable.

Note that in a phase-separated state we have the droplets (clusters) with a density ratio n_h/n_l that is higher or lower than the density ratio in a homogeneous state. For example, in a fully phase-separated state we have two large clusters (1,2) with $n_{h1} > n_h > n_{h2}$. Thus Eq. (93) for the effective interaction is valid for both clusters but with local values of p_{Fh}/p_{Fl} . Correspondingly, the critical temperature will be different for these two clusters at least in the zero approximation when we neglect Josephson coupling or the proximity effect between the neighboring clusters or droplets.

Similarly, an effective interaction (irreducible bare vertex) for light electrons in the Cooper channel has the form

$$V_{\text{eff}}(\mathbf{p}_l, \mathbf{p}'_l) = T_{ll} + T_{ll}^2 \Pi_{ll}(0, \tilde{\mathbf{q}}_l = \mathbf{p}_l + \mathbf{p}'_l) - 2T_{hl}^2 \Pi_{hh}(0, \mathbf{q}_l = \mathbf{p}_l - \mathbf{p}'_l), \quad (98)$$

where $|\mathbf{p}_l| = |\mathbf{p}'_l| = p_{Fl}$ and $\tilde{q}_l \leq 2p_{Fl}$; and, $q_l \leq 2p_{Fl}$ for SC.

$$\tau_{ll} = \frac{4\pi}{m_h^* \ln(1/p_{Fh}^2 d^2)} > 0$$

is a T -matrix for the light electrons. Using the expressions

$$\begin{aligned} \Pi_{ll}(0, \tilde{\mathbf{q}}_l) &= Z_l^2 \frac{m_l}{2\pi} \left[1 - \text{Re} \sqrt{1 - \frac{4p_{Fl}^2}{\tilde{q}_l^2}} \right], \\ \Pi_{hh}(0, \mathbf{q}_l) &= Z_h^2 \frac{m_h}{2\pi} \left[1 - \text{Re} \sqrt{1 - \frac{4p_{Fh}^2}{q_l^2}} \right], \end{aligned} \quad (99)$$

and given that $p_{Fl} > p_{Fh}$, we obtain

$$V_{\text{eff}}(\mathbf{p}_l, \mathbf{p}'_l) \approx T_{ll} + T_{ll}^2 \frac{m_l}{2\pi} - 2 \frac{m_h}{2\pi} Z_h^2, \quad (100)$$

where we have set $Z_l \sim m_l^*/m_l \sim 1$.

Thus, an effective interaction for the light electrons does not contain any nontrivial dependence on \mathbf{q}_l and $\tilde{\mathbf{q}}_l$, so that superconductivity with $m \neq 0$ does not exist for light electrons in this approximation. Note that s -wave pairing for light electrons is also suppressed by the first order term $T_{ll} > 0$ in V_{eff} (98).

However, adding a Suhl term,^{33,34} which is related to rescattering of Cooper pairs between the bands,

$$K(a_p^+ a_{-p}^+ b_p b_{-p'} + \text{h.c.}) \quad (101)$$

to the Hamiltonian of the two-band model (2) makes the light band superconductive at the same temperature as the heavy one, even for infinitely small K. Thus T_{c1} in Eq. (91) is a mutual SC temperature for the two-band model with one narrow band.¹²

XVIII. DISCUSSION AND CONCLUSIONS

We have analyzed the characteristic features of a two-band Hubbard model with one narrow band taking electron-electron scattering into account for the clean case (no impurities) with low electron densities. We considered the

electron-polaron effect and other mechanisms for heavy mass enhancement related to the momentum dependence of the self energies.

In the 3D-case the dominant mechanism for heavy mass enhancement is related to the momentum-dependence of the real part of the “heavy-light” self-energy and leads to linear (in the mass-ratio) renormalization of the heavy mass. In 2D, the dominant mechanism for heavy mass enhancement is EPE, which leads to logarithmic renormalization of the heavy particle Z -factor. In the unitary limit if we start with $m_h/m_l \sim 10$ for the bare-mass ratio in the LDA scheme we can end up with $m_h^*/m_l \sim 100$ owing to many-body effects; this is quite natural for uranium-based HF systems.

The important role of the interband (“heavy-light”) Hubbard repulsion U_{hl} for formation of a heavy mass $m^* \sim 100m_e$ in a two-band Hubbard model has also been noted³⁵ for the HF compound LiV_2O_4 . For a large density mismatch $n_h \gg n_l$ we can see a tendency towards negative compressibility in a heavy band in the strong coupling limit $f_0^2 m_h p_{Fh} / m_l p_{Fl} \gg 1$ even at low densities, which can lead to redistribution of charge between the bands and, possibly, to nanoscale phase separation that is qualitatively similar to that reported in Ref. 10. The tendency towards phase-separation at low electron densities also shows up in the asymmetric Hubbard model (which possesses Hubbard repulsion between heavy and light electrons) in the limit of strong asymmetry $t_h \ll t_l$ ³⁶ between the heavy and light bandwidths.

For equal densities of heavy and light bands the resistivity in a homogeneous state behaves as a Fermi liquid, with $R(T) \propto T^2$ at low temperatures $T < W_h^*$ in both 3D and 2D (where W_h^* is an effective bandwidth of the heavy particles).

At higher temperatures $T > W_h^*$, when coherent motion of particles in the heavy band is totally destroyed, the heavy particles move diffusively among the surrounding light particles while the light particles scatter on the heavy ones as on immobile (static) impurities. The resistivity approaches saturation in 3D, which is typical for some uranium-based HF-compounds including UNi_2Al_3 .

In 2D, because of weak-localization Altshuler-Aronov corrections, the resistivity at higher temperatures has a maximum and then a localization tail. Such behavior could be also relevant in some other mixed-valence systems, possibly including layered manganites. A similar behavior with a metallic dependence for the resistivity at low temperatures $T < 130$ K and an insulator-like dependence at high temperatures has also been observed in layered intermetallic Gd_5Ge_4 alloys;³⁸ there³⁸ a strongly-correlated narrow band was assumed to exist at low temperatures.

We have briefly discussed the SC-instabilities which arise in this model at low electron densities. The leading instability, of an enhanced Kohn–Luttinger type, corresponds to p -wave pairing of heavy electrons via polarization of light electrons. In the quasi-2D case, T_c can reach experimentally realistic values even at low densities in the layered dichalcogenides CuS_2 and CuSe_2 and in InAs-GaSb and PbTe-SnTe semimetallic superlattices with geometrically separated bands belonging to neighboring layers.³⁹ Note that p -wave SC has been widely discussed for 3D heavy-fermion systems such as $\text{U}_{1-x}\text{Th}_x\text{Be}_{13}$ ⁴⁰ and the layered ruthenates Sr_2RuO_4 with several pockets (bands) for conducting electrons.⁴¹ Note

also that when we increase the density of a heavy band and approach half-filling ($n_h \rightarrow 1$), d -wave superconductive pairing (as in UPt_3) becomes more beneficial in the heavy band in terms of the spin-fluctuation theory.^{42,43} Different mechanisms for SC in HF-compounds, including odd-frequency pairing, have been discussed by P. Coleman, *et al.*⁴⁸

Note also that if we study the orbitally degenerate two band Hubbard model, then the Hubbard parameters become $U = U_{hh} = U_{ll} - U_{hl} + 2J_H$ (where J_H is Hund’s coupling).⁴⁴ Near half-filling this model becomes equivalent to the t - J orbital model;⁴⁵ for $J < t$ and at optimal doping it contains SC d -wave pairing⁴⁶ governed by superexchange interaction between different orbitals of AFM-type $J > 0$. Note that, when t_h and t_l do not differ greatly, typically we have $J \sim t^2/U \sim 300$ K. The orbital t - J model also reveals a tendency towards nanoscale phase-separation at low doping,⁴⁷ with the creation of orbital ferrons inside an insulating AFM orbital matrix. An orbital type of phase-separation may have been observed in URu_2Si_2 .³⁷

Finally, it is interesting to note that the electron specific heat in the homogeneous state of the two-band model with one narrow band for $T_c < T < W_h^*$ behaves linearly in T , i.e., $C_v \propto n_h(T/W_h^*)$, while for $W_h^* < T < W_l$ the specific heat decreases as $C_v \propto n_h(W_h^*/T)^2$.¹ Thus, it has a maximum at $T \sim W_h^*$ in a mixed-valence regime of the two-band model.

We thank A.S. Alexandrov, A.F. Andreev, M.A. Baranov, Yu. Bichkov, A.V. Chubukov, D.V. Efremov, A.S. Hewson, K.A. Kikoin, F.V. Kusmartsev, P. Nozieres, T.M. Rice, A.O. Sboychakov, P. Thalmeier, C.M. Varma, D. Vollhardt, P. Woelfle, A. Yaresko and, especially, P. Fulde, Yu. Kagan, K.I. Kugel, and N.V. Prokof’ev for many simulating discussions on this subject and acknowledge the financial support of RFBR grants # 08-02-00224 and 08-02-00212. M.Yu.K. is also grateful to the Leverhulme trust for a grant to visit Loughborough University, where this work was completed.

^aEmail: kagan@kapitza.ras.ru

¹Yu. Kagan and N. V. Prokof’ev, Sov. Phys. JETP **93**, 356 (1987); Yu. Kagan and N. V. Prokof’ev, Sov. Phys. JETP **90**, 2176 (1986).

²J. Kondo, Prog. Theor. Phys. **32**, 37 (1964); C. M. Varma and Y. Yaflet, Phys. Rev. B **13**, 2959 (1976); A. C. Hewson, The Kondo Problem to Heavy Fermions, Cambridge University Press, Cambridge (1993).

³A. M. Tsvelik and P. B. Wiegman, Adv. Phys. **32**, 453 (1983); N. Andrei, F. Furuya, and J. H. Loerenstein, Rev. Mod. Phys. **55**, 331 (1983).

⁴D. M. Newns and M. Read, Adv. Phys. **56**, 799 (1987); P. Coleman, Phys. Rev. B **35**, 5072 (1987); C. M. Varma, arXiv:cond-mat/0510019 (2005).

⁵C. M. Varma, P. B. Littlewood, S. Schmitt-Rink, E. Abrahams, and A. E. Ruchenstein, Phys. Rev. Lett. **63**, 1996 (1989).

⁶J. S. Kim, B. Andraka, and G. R. Stewart, Phys. Rev. B **45**, 12081 (1992).

⁷A. L. Altshuler and A. G. Aronov, in: Modern Problems in Condensed Matter Systems, North Holland, Amsterdam (1985), v. 10, p. 1.

⁸M. Yu. Kagan, A. G. Aronov, and Checkoslov, J. Phys. **46**, 2061 (1996), Proc. LT-21 Conference, Prague (1996).

⁹A. L. Rakhmanov, K. I. Kugel, Ya. M. Blanter, and M. Yu. Kagan, Phys. Rev. B **63**, 174424 (2001); M. Yu. Kagan and K. I. Kugel, Sov. Phys. Usp. **171**, 577 (2001).

¹⁰K. I. Kugel, A. L. Rakhmanov, and A. O. Sboychakov, Phys. Rev. B **76**, 195113 (2007).

¹¹M. Yu. Kagan and A. V. Chubukov, JETP Lett. **47**, 525 (1988); M. A. Baranov, A. V. Chubukov, and M. Yu. Kagan, Int. J. Mod. Phys. B **6**, 2471 (1992); M. A. Baranov, D. V. Efremov, M. S. Mar’enko, and M. Yu. Kagan, Sov. Phys. JETP **90**, 861 (2000).

- ¹²M. Yu. Kagan, Phys. Lett. A **152**, 303 (1991); M. A. Baranov and M. Yu. Kagan, Sov. Phys. JETP **102**, 313 (1991).
- ¹³W. Kohn and J. M. Luttinger, Phys. Rev. Lett. **15**, 524 (1965).
- ¹⁴J. Kanamori, Prog. Theor. Phys. **30**, 275 (1963); J. Hubbard, Proc. R. Soc. London, Ser. A **276**, 235 (1963).
- ¹⁵V. M. Galitskii, Sov. Phys. JETP **34**, 151 (1958).
- ¹⁶E. M. Lifshitz and L. P. Pitaevskii, Statistical Physics, Nauka, Moscow (1973), Pt. 2.
- ¹⁷P. Bloom, Phys. Rev. B **12**, 125 (1975).
- ¹⁸A. A. Abrikosov, L. P. Gor'kov, and I. E. Dzyaloshinskii, Methods of Quantum Field Theory in Statistical Physics, Dover, New York (1975).
- ¹⁹M. Yu. Kagan and P. Woelfle, unpublished.
- ²⁰P. W. Anderson, Phys. Rev. Lett. **64**, 1839 (1990); P. W. Anderson, Phys. Rev. Lett. **65**, 2306 (1990); P. W. Anderson, Phys. Rev. Lett. **66**, 3226 (1991).
- ²¹J. R. Engelbrecht and M. Randeria, Phys. Rev. Lett. **65**, 1032 (1990); J. R. Engelbrecht and M. Randeria, Phys. Rev. Lett. **66**, 3225 (1990); J. R. Engelbrecht and M. Randeria, Phys. Rev. B **45**, 12419 (1992).
- ²²M. Yu. Kagan, Superconductivity and Superfluidity in Fermi-Systems with Repulsive Interaction, Habilitation Thesis, P.L. Kapitza Institute for Physical Problems, Moscow (1994).
- ²³M. Yu. Kagan and N. V. Prokof'ev, unpublished.
- ²⁴G. Iche and P. Nozieres, Physica A **91**, 485 (1978); P. Nozieres and L. T. de Dominicis, Phys. Rev. **178**, 1097 (1969).
- ²⁵P. W. Anderson, Phys. Rev. Lett. **18**, 1049 (1958); P. W. Anderson, Phys. Rev. B **164**, 352 (1967).
- ²⁶R. M. White and P. Fulde, Phys. Rev. Lett. **47**, 1540 (1981); G. Zwicknagl, A. Yaresko, and P. Fulde, Phys. Rev. B **68**, 052508 (2003); G. Zwicknagl, A. Yaresko, and P. Fulde, Phys. Rev. B **65**, 081103 (2002); M. Koga, W. Liu, M. Dolg, and P. Fulde, Phys. Rev. B **57**, 10648 (1998); P. Fulde, Electron Correlations in Molecules and Solids, Springer, Berlin (1995).
- ²⁷Yu. Kagan, K. A. Kikoin, and N. V. Prokof'ev, JETP Lett. **56**, 221 (1992).
- ²⁸I. M. Lifshitz and A. M. Kosevich, Zh. Eksp. Teor. Fiz. **29**, 730 (1955); D. Schoenberg, Magnetic Oscillations in Metals, Mir, Moscow (1986); L. Taillefer and G. G. Lonzarich, Phys. Rev. Lett. **60**, 1570 (1988); A. Wasserman, M. Springford, and A. C. Hewson, J. Phys.: Condens. Matter **1**, 2669 (1989).
- ²⁹T. Ito, H. Kumigashira, H.-D. Kim, T. Takahashi, N. Kimura, Y. Haga, E. Yamamoto, Y. Onuki, and H. Harima, Phys. Rev. B **59**, 8923 (1999); A. J. Arko, J. J. Joyce, A. B. Andrews, J. D. Thompson, J. L. Smith, E. Moshopoulou, Z. Fisk, A. A. Menovsky, P. C. Canfield, and C. G. Olson, Physica B **230–232**, 16 (1997).
- ³⁰A. Berton, J. Chaussy, B. Cornut, J. Flouquet, J. Odin, J. Peyrard, and F. Holtzberg, Phys. Rev. B **23**, 3504 (1981); G. R. Stewart, Rev. Mod. Phys. **56**, 755 (1984); H. R. Ott, Sov. J. Low Temp. Phys. **11**, 215 (1987).
- ³¹E. M. Lifshitz and L. P. Pitaevskii, Physical Kinetics, Nauka, Moscow (1979); L. D. Landau, Phys. Z. Sov. **10**, 154 (1936).
- ³²Y. Imry, Introduction to Mesoscopic Physics, Oxford University Press, Oxford (2002); Y. Aharonov and D. Bohm, Phys. Rev. **115**, 485 (1959).
- ³³H. Suhl, T. B. Matthias, and L. R. Walker, Phys. Rev. Lett. **3**, 552 (1959).
- ³⁴B. T. Geilikman, Sov. Phys. JETP **21**, 796 (1965); B. T. Geilikman, Phys. Usp. **88**, 327 (1966); B. T. Geilikman, Phys. Usp. **109**, 65 (1973).
- ³⁵H. Kusunose, S. Yotsuhashi, and K. Miyake, Phys. Rev. B **62**, 4403 (2000).
- ³⁶P. Farkašovský, Phys. Rev. B **77**, 085110 (2008).
- ³⁷P. Chandra, P. Coleman, J. A. Mydosh, and V. Tripathi, Nature **417**, 831 (2002); P. Chandra, P. Coleman, J. A. Mydosh, and V. Tripathi, J. Phys.: Condens. Matter **15**, S1965 (2003).
- ³⁸E. M. Levin, V. K. Pecharsky, K. A. Gschneidner, Jr., and G. J. Miller, Phys. Rev. B **64**, 235103 (2001).
- ³⁹K. Murase, S. Ishida, S. Takaoka, T. Okumura, H. Fujiyasu, A. Ishida, and M. Aoki, Surf. Sci. **170**, 486 (1986).
- ⁴⁰F. Steglich, J. Aarts, C. D. Bredl, G. Cordier, F. R. de Boer, W. Lieke, and U. Rauchschwalbe, in: Superconductivity in d and f-band metals, Kernforschungszentrum, Karlsruhe (1982); M. Sigrist and K. Ueda, Rev. Mod. Phys. **63**, 239 (1991).
- ⁴¹Y. Maeno, T. M. Rice, and M. Sigrist, Phys. Today **54**, 42 (2001); T. M. Rice and M. Sigrist, J. Phys.: Condens. Matter **7**, L643 (1995).
- ⁴²D. J. Scalapino, E. Loh, Jr., and J. E. Hirsch, Phys. Rev. B **34**, 8190 (1986).
- ⁴³K. Miyake, S. Schmitt-Rink, and C. M. Varma, Phys. Rev. B **34**, 6554 (1986).
- ⁴⁴K. I. Kugel and D. I. Khomskii, Sov. Phys. Usp. **136**, 621 (1982).
- ⁴⁵S. Ishihara, J. Inoue, and S. Maekawa, Phys. Rev. B **55**, 8280 (1997).
- ⁴⁶M. Yu. Kagan and T. M. Rice, J. Phys.: Condens. Matter **6**, 3771 (1994).
- ⁴⁷K. I. Kugel, A. L. Rakhmanov, A. O. Sboychakov, and D. I. Khomskii, Phys. Rev. B **78**, 115113 (2008).

This article was published in English in the original Russian journal. Reproduced here with stylistic changes by AIP.